J. Fluid Mech. (1978), *vol.* 88, *part* 4, *pp.* 641–657
Printed in Great Britain

Blast-wave propagation in a spray

By T. H. PIERCE

Department of Mechanical and Aerospace Engineering,
North Carolina State University, Raleigh†

(Received 20 July 1977)

A first-order analysis is presented for the propagation of a blast wave through a dilute spray of non-reactive liquid droplets that are suspended in a non-reactive gas-phase carrier. The analysis permits straightforward computation of decay rates and internal wave structure for wave strengths in the approximate Mach number range $4 \leqslant M_s \leqslant 15$, and loading factors (mass of spray per unit mass of carrier) less than about 0·4. The droplets must be sufficiently small to completely change phase in a distance behind the shock that is at all times negligible compared with the wave radius. Representative calculations are presented and discussed. These show more rapid decay rates and higher pressures, densities, and particle velocities in two-phase blast waves when compared against equivalent gas-phase blast waves. A simplification of the analysis for the regime of higher wave Mach numbers (strong waves) is also given, which for that case allows direct algebraic calculation of early wave characteristics.

1. Introduction

If the thermal energy content of a relatively small region within a larger volume of non-reactive gas is increased slowly by external means, the result is an essentially quiescent spreading of this thermal energy throughout the gas. On the other hand, if the rate of external energy addition is so fast as to overwhelm the combined rates of thermal conduction and radiation, a 'blast wave' results. In this latter case as energy is added it initially accumulates within the small region ('explosion centre') so that the pressure and temperature there are increased. The resulting unbalanced pressure gradient between the explosion centre and neighbouring layers of gas produces a finite-strength compression wave that propagates away from the centre. The shock wave that is ultimately developed accelerates gas particles in the same direction. However, for symmetrical geometries, the gas particle velocity at the centre itself must be zero, and therefore an expansion wave forms in the gas between the shock and the explosion centre. This expansion wave continuously interacts with the shock, so that after the external energy deposition has ceased the shock steadily diminishes to a Mach wave.

The simplest analytic model of a gas-phase blast wave treats the explosion centre as a point, line, or plane (in spherical, cylindrical, or planar geometries). The gas is taken to be in a uniform thermodynamic state (initially) and to be thermally and calorically perfect and chemically inert. All of the externally added energy is assumed to be deposited in zero time, and the subsequent flow is analysed only for the period

† Present address: Systems, Science and Software, P.O. Box 1620, La Jolla, California 92038.

during which the shock is very strong (pressure increase across the shock is large). A description of this model is given for example by Sedov (1959).

Refinements of this model have included consideration of the latter stages of wave decay (weak blast wave), discussed for example by Korobeinikov (1971) and Sakurai (1965); the effects of non-instantaneous energy deposition, described by Woolfolk & Ablow (1974), Dabora (1972), and others; propagation through an initial atmosphere having non-uniform thermodynamic state, given by Treve & Manley (1972); and so forth. Recent studies have explored blast-wave propagation in reactive gas mixtures, in connexion with the direct initiation of gas-phase detonations, for example Bach, Knystautas & Lee (1971).

The present paper deals with the first-order characteristics of blast-wave propagation through a medium comprising non-reactive liquid droplets that are suspended in a non-reactive gaseous 'carrier'. The initial energy deposition is assumed to be instantaneous, into an explosion centre of vanishing radial size. A principal assumption requires that the droplets be completely broken up and vaporized in a distance that is small compared with the blast-wave radius at any instant. This assumption immediately constrains the maximum allowable droplet size, or the maximum and minimum wave strengths that can be accommodated by this development. This and other key assumptions will be discussed in detail in §5.

2. Analysis of shock discontinuity

The fluid characteristics just downstream of the shock serve as boundary conditions for the flow within the blast wave. In the present context the 'shock' includes the droplet breakup and vaporization zone. This is illustrated in figure 1. It is necessary to determine conditions at point 3 in terms of those at point 1.

For a stationary control volume connecting points 1 and 3, and with the frame of reference fixed to the shock, steady-state mass, momentum and energy conservation are, respectively,

$$\dot{m}_s + \dot{m}_c = \dot{m}_3, \tag{1}$$

$$P_1 A + \dot{m}_s u_1 + \dot{m}_c u_1 = P_3 A + \dot{m}_3 \hat{u}_3, \tag{2}$$

$$\dot{m}_c(e_{c1} + u_1^2/2) + \dot{m}_s(e_{s1} + u_1^2/2) + P_1 A u_1 = \dot{m}_c(e_{c3} + \hat{u}_3^2/2) + \dot{m}_s(e_{s3} + \hat{u}_3^2/2) + P_3 A \hat{u}_3. \tag{3}$$

Here the subscripts s and c refer to the species that is initially in condensed form, and the carrier; P, u, e and $\dot{m}$ designate pressure, velocity, internal energy, and mass flow rate; $\hat{u}_3$ denotes the *shock-relative* velocity at point 3; and A is an arbitrary flow cross-sectional area. Gas/vapour mixture characteristics at point 3 are represented by P_3, $\hat{u}_3$, $\dot{m}_3$, etc.

Assuming that the droplets themselves exert negligible pressure, then $P_{s1} = 0$ and so $P_1 \doteq P_{c1}$. If the initial carrier pressure is not large, the values of internal energy and enthalpy of the liquid will be nearly equal; i.e. $e_{s1} \doteq h_{s1}$. Moreover, at low pressure the initial enthalpy of the liquid will very nearly equal the saturated liquid value at the initial temperature, T_1.

It is further assumed that the initially condensed species behaves as a thermally and calorically (constant specific heats) perfect gas when in the vapour phase, as does the carrier, and that the droplets and carrier possess the same initial temperature.

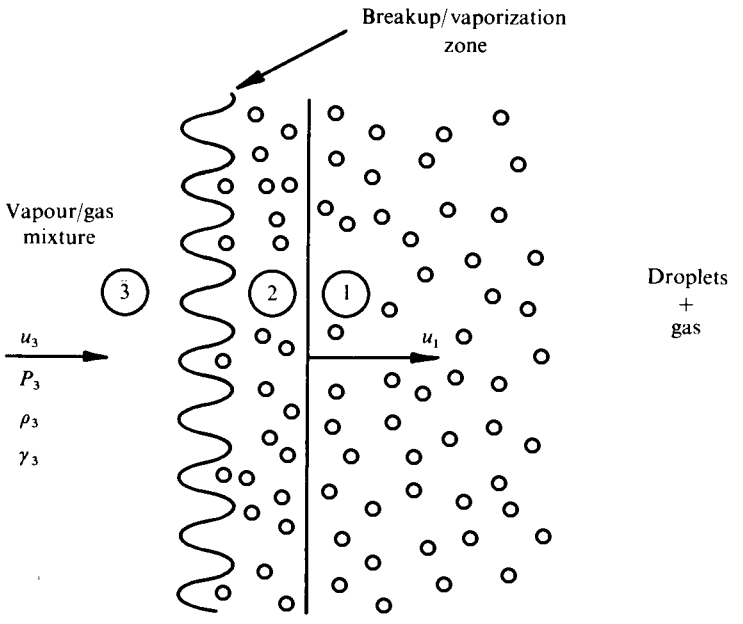

FIGURE 1. Schematic of blast wave shock in ground-fixed co-ordinates.

Then, if the gas/vapour mixture at point 3 behaves as a Dalton gas so that $P_3 = P_{c3} + P_{s3}$, the conservation equations can be written as

$$\phi \rho_{c1} u_1 = \rho_3 \hat{u}_3, \tag{4}$$

$$P_1 + \phi \rho_{c1} u_1^2 = P_3 + \rho_3 \hat{u}_3^2, \tag{5}$$

and

$$\frac{a_1^2}{\gamma_c - 1} - \omega_s (L_1 - C_{ps} T_1) + \tfrac{1}{2} \phi u_1^2 = \phi \left(\frac{a_3^2}{\gamma_3 - 1} + \frac{\hat{u}_3^2}{2} \right). \tag{6}$$

In these equations, ρ designates density, ω_s is the 'loading factor'† defined by

$$\omega_s \equiv \dot{m}_s / \dot{m}_c,$$

a is the speed of sound, L_1 is the heat of vaporization of the liquid at initial temperature T_1, C_{ps} is the *vapour-phase* constant-pressure specific heat of the initially-condensed species, and $\phi \equiv 1 + \omega_s$. The sound speed at point 1 is computed from

$$a_1^2 = \frac{\gamma_c P_{c1}}{\rho_{c1}},$$

where γ_c is the ratio of specific heats for the carrier. The effect on a_1 of the presence of the droplets is ignored. The speed of sound in the mixture at point 3 is simply $a_3^2 = \gamma_3 P_3 / \rho_3$ where γ_3 is the specific heats ratio at point 3. The value of γ_3 is easily shown to be

$$\gamma_3 = \gamma_c \left(\frac{1 + \omega_s \bar{C}_p}{1 + \bar{\gamma} \omega_s \bar{C}_p} \right),$$

† Note that the loading factor simply represents the mass of liquid per unit mass of carrier in any fixed volume. Downstream of the shock, with the initially condensed species in the vapour phase, the loading factor is identical with what is commonly called the 'humidity ratio'. The volume occupied by the droplets is neglected in this analysis.

where $\bar{C}_p \equiv C_{ps}/C_{pc}$, $\bar{\gamma} \equiv \gamma_c/\gamma_s$ and γ_s is the vapour-phase value for the initially condensed species. Conservation of mass by species can be used to show that the fractional composition, and therefore the loading factor, is the same at points 1 and 3.

A solution to (4)–(6) is

$$\hat{u}_3/u_1 = \phi(\rho_{c1}/\rho_3), \tag{7}$$

and

$$P_3/P_1 = 1+\zeta(\rho_{c1}/\rho_3)\,(\rho_3/\rho_{c1}-\phi), \tag{8}$$

where

$$\frac{\rho_3}{\rho_{c1}} = \frac{\phi\left\{\left(\frac{\gamma_3}{\gamma_3-1}\right)(1+\zeta)+\left(\left[\frac{\gamma_3}{\gamma_3-1}\right]^2(1+\zeta)^2-2\zeta\left[\left(\frac{\gamma_c}{\gamma_c-1}\right)-\gamma_c\omega_s\epsilon+\tfrac{1}{2}\zeta\right]\left[\frac{\gamma_3+1}{\gamma_3-1}\right]\right)^{\frac{1}{2}}\right\}}{2\left[\left(\frac{\gamma_c}{\gamma_c-1}\right)-\gamma_c\omega_s\epsilon+\tfrac{1}{2}\zeta\right]}, \tag{9}$$

in which

$$\zeta \equiv \phi\gamma_c u_1^2/a_1^2,$$

$$\epsilon \equiv \bar{L}-\bar{C}_p/(\gamma_c-1),$$

and

$$\bar{L} \equiv L_1/a_1^2.$$

This form for the shock solution is too complex to be used tractably in conjunction with the blast-wave equations. For this reason it is now assumed that the radicand in (9) can be replaced by

$$\left(\frac{\zeta-\gamma_3}{\gamma_3-1}\right)^2,$$

an approximation that formally requires $\gamma_3 \doteq \gamma_c$ and $|2\gamma_3\zeta\omega_s\epsilon(\gamma_3^2-1)/(\zeta-\gamma_3)^2| \ll 1$ (a dilute spray or strong shock). Equations (7)–(9) simplify to

$$\hat{u}_3/u_1 = \alpha_2\{(\mu/\alpha_1 M_s^2\phi)+1\}, \tag{10}$$

$$P_3/P_1 = \gamma_c M_s^2\phi(1-\alpha_2)-(\gamma_c\mu\alpha_2/\alpha_1)+1, \tag{11}$$

$$\rho_3/\rho_1 = \alpha_1\phi^2 M_s^2/\alpha_2(\mu+\alpha_1 M_s^2\phi), \tag{12}$$

where $M_s = u_1/a_1$ is the shock Mach number, and

$$\alpha_1 \equiv \gamma_c-1, \quad \alpha_2 \equiv (\gamma_3-1)/(\gamma_3+1), \quad \mu \equiv 2[1-(\gamma_c-1)\,\omega_s\epsilon].$$

3. Blast-wave analysis

The unsteady gas motion between the shock front and the centre of explosion is considered to be inviscid so that the Euler equations can be used. These are

$$\frac{\partial\rho}{\partial t}+u\frac{\partial\rho}{\partial r} = -\rho\left(\frac{\partial u}{\partial r}+\frac{\alpha u}{r}\right) \qquad \text{(mass)}, \tag{13}$$

and

$$\frac{\partial u}{\partial t}+u\frac{\partial u}{\partial r} = -\frac{1}{\rho}\frac{\partial P}{\partial r} \qquad \text{(momentum)}. \tag{14}$$

Radius r is measured from the explosion centre along a streamline. The value of α is 0, 1, or 2 for planar, cylindrical, and spherical geometries, respectively. The energy equation is not included since it will be replaced by a forthcoming assumption.

The 'blast-wave radius' R is the distance between the shock and explosion centre. It is of course a function of time t, described by

$$dR(t)/dt = u_1(t).$$

The boundary conditions are obtained directly from (10)–(12). That is,

$$P(R,t) = P_3(t), \quad u(R,t) = u_3(t), \quad \rho(R,t) = \rho_3(t).$$

The relation between absolute (ground-relative) velocity u_3 and shock-relative velocity $\hat{u}_3$ is simply $u_3 = u_1 - \hat{u}_3$. The initial conditions are $R = 0$ and $M_s \to \infty$ at $t = 0$. These reflect the instantaneous deposition of a finite quantity of energy into zero volume, producing an infinite pressure rise there, in the first moment.

The solution to this problem which follows parallels the approximate analysis given by Sakurai (1965) for gas-phase blast waves. Accordingly, new dependent variables f, g, and h, and new independent variables x and y are introduced. These are

$$f(x,y) \equiv u/u_1, \quad g(x,y) \equiv yP/P_1, \quad h(x,y) \equiv \rho/\rho_{c1},$$

and

$$x \equiv r/R, \quad y \equiv M_s^{-2}.$$

In this way, with the further definition

$$\lambda \equiv \frac{R}{y}\frac{dy}{dR},$$

the differential equations (13) and (14) become, respectively,

$$(f-x)\frac{\partial h}{\partial x} + \lambda y \frac{\partial h}{\partial y} = -h\left(\frac{\partial f}{\partial x} + \frac{\alpha f}{x}\right), \tag{15}$$

$$-\tfrac{1}{2}\lambda f + (f-x)\frac{\partial f}{\partial x} + \lambda y \frac{\partial f}{\partial y} = -\frac{1}{\gamma_c h}\frac{\partial g}{\partial x}, \tag{16}$$

while the boundary conditions transform to

$$f(1,y) = 1 - \alpha_2\{(\mu y/\alpha_1\phi) + 1\}, \tag{17}$$

$$g(1,y) = \gamma_c\phi(1-\alpha_2) + y\{1 - (\gamma_c\mu\alpha_2/\alpha_1)\}, \tag{18}$$

and

$$h(1,y) = \alpha_1\phi^2/(\mu\alpha_2 y + \alpha_1\alpha_2\phi). \tag{19}$$

It is now assumed that

$$f(x,y) = f_0(y)\,x; \tag{20}$$

that is, at any time t the velocity is taken to be a linear function of radius (whose value is u_3 at the shock, $r = R$, and zero at the explosion centre, $r = 0$). This assumption circumvents the need for the Euler energy equation.

The function $f_0(y)$ can immediately be obtained by applying the boundary condition (17), to the value of f at $x = 1$. This gives.

$$f_0 = 1 - \alpha_2\{(\mu y/\alpha_1\phi) + 1\}. \tag{21}$$

Equation (15) can then be readily integrated if the values of $\lambda y\,\partial h/\partial y$ are assumed to be small by comparison with $(f-x)\,\partial h/\partial x$ for all (x,y). If this assumption is adopted, then after substituting (20) into (15) and integrating,

$$h = h_0(y)\,x^m, \tag{22}$$

where

$$m \equiv f_0(\alpha+1)/(1-f_0). \tag{23}$$

The function $h_0(y)$ is obtained by applying (19), the boundary condition at $x = 1$, to (22). By this procedure it is found that

$$h_0 = \phi/[(\mu\alpha_2 y/\alpha_1\phi)+\alpha_2]. \tag{24}$$

Now (16) can be integrated over x, after substituting (20) and (22). The constant of integration is evaluated by invoking the boundary condition, (18). The result is

$$g = A(x^{m+2}-1)+g_0, \tag{25}$$

where

$$A \equiv \frac{\gamma_c h_0}{m+2}\left[f_0(1+\tfrac{1}{2}\lambda-f_0)+\frac{\lambda y\alpha_2\mu}{\alpha_1\phi}\right], \tag{26}$$

and

$$g_0 \equiv \gamma_c\phi(1-\alpha_2)+y(1-(\gamma_c\mu\alpha_2/\alpha_1)). \tag{27}$$

Simple algebraic forms for the distributions in P, ρ, and u within the wave are thus obtained. However, values for g cannot be determined nor can $M_s = M_s(R)$ be found until the function $\lambda(y)$ is known.

The additional physical equation that is required in order to evaluate $\lambda(y)$ is supplied by integral energy conservation. It is argued that, at any time $t > 0$ (when the blast-wave radius is R), the total energy content within the region $0 \leqslant r \leqslant R$ must exceed that contained within the same region for $t < 0$ by an amount that is equal to the energy deposited at the explosion centre at $t = 0$. That is, the shock represents the only mechanism which carries energy away from the centre. Hence,

$$\int_0^R [\rho_c(e_c+u^2/2)+\rho_s(e_s+u^2/2)]\,r^\alpha\,dr = \int_0^R [\rho_{c1}e_{c1}+\rho_{s1}e_{s1}]\,r^\alpha\,dr + E_\alpha, \tag{28}$$

where E_α is defined as: deposited energy per unit area, for $\alpha = 0$ (planar); deposited energy per unit length divided by 2π, for $\alpha = 1$ (cylindrical); and deposited energy divided by 4π, for $\alpha = 2$ (spherical).

Equation (28) is simplified by using the same assumptions that were employed in reducing the jump equations for the shock-wave analysis in §2 (prior to solving). Additionally, integral conservation of mass by species for the region $0 \leqslant r \leqslant R$, between $t < 0$ and any $t > 0$, is needed; i.e.

$$\int_0^R (\rho_c-\rho_{c1})\,r^\alpha\,dr = 0,$$

and

$$\int_0^R (\rho_s-\rho_{s1})\,r^\alpha\,dr = 0.$$

After considerable rearrangement (28) then becomes

$$E_\alpha = \int_0^R \left(\tfrac{1}{2}\rho u^2+\frac{P}{\gamma_3-1}\right) r^\alpha\,dr - \frac{\theta P_1 R^{\alpha+1}}{(\alpha+1)(\gamma_c-1)}, \tag{29}$$

where

$$\theta \equiv 1-\gamma_c(\gamma_c-1)\,\omega_s\epsilon.$$

If the dimensionless variables f, g, h, x, y are introduced into (29) along with the characteristic radius

$$R_0 \equiv (E_\alpha/P_1)^{1/(\alpha+1)}, \tag{30}$$

then

$$y(R_0/R)^{\alpha+1} = J(y)-[\theta y/(\gamma_c-1)(\alpha+1)], \tag{31}$$

in which

$$J(y) \equiv \int_0^1 \left(\tfrac{1}{2}\gamma_c h f^2+\frac{g}{\gamma_3-1}\right) x^\alpha\,dx. \tag{32}$$

Substituting (20), (22) and (25) into (32) then leads to

$$J(y) = S(y) + \lambda Q(y), \tag{33}$$

where

$$S \equiv \frac{\gamma_c h_0 f_0}{m+3+\alpha}\left[\frac{f_0}{2} + \frac{(1-f_0)}{(m+2)(\gamma_3-1)}\right] + \frac{1}{(\gamma_3-1)(\alpha+1)}\left[g_0 - \frac{\gamma_c h_0 f_0}{m+2}(1-f_0)\right]$$

and

$$Q \equiv \frac{\gamma_c h_0}{(m+2)(\gamma_3-1)}\left(\frac{f_0}{2} + \frac{\mu\alpha_2 y}{\alpha_1 \phi}\right)\left(\frac{1}{m+3+\alpha} - \frac{1}{\alpha+1}\right).$$

The required function $\lambda(y)$ is obtained by solving (33), giving

$$\lambda = (J-S)/Q, \tag{34}$$

which can be evaluated once $J(y)$ is known.

The function $J(y)$ cannot unfortunately be determined directly from (31), since $R(y)$ is not yet known. However, if (31) is differentiated with respect to y,

$$\frac{dJ}{dy} = \frac{J}{y}\left(1 - \frac{\alpha+1}{\lambda}\right) + \frac{\theta}{(\gamma_c-1)\lambda}. \tag{35}$$

This equation can be subsequently re-integrated numerically beginning from $y = 0$ ($t = 0$), to yield $J = J(y)$. Once $J(y)$ is known, $\lambda(y)$ is calculated from (34), and then $R(y)$ can be determined from (31); i.e.

$$\frac{R}{R_0} = \left[\frac{J}{y} - \frac{\theta}{(\gamma_c-1)(\alpha+1)}\right]^{-1/(\alpha+1)}. \tag{36}$$

Thus, the principal arithmetic task required by this approximate formulation is the integration of (35). For that purpose, initial values for λ and J are required. The initial conditions are $y = 0$ at $R = 0$, and, since $J(0)$ is necessarily finite, solving (35) for λ and setting $y = 0$ shows that $\lambda(0) = \alpha + 1$.

Although the value of $J(0)$ can then be computed directly from (33), the value of the derivative, dJ/dy at $y = 0$, is indeterminate. This can be clearly seen from (35). Application of L'Hospital's Rule to the first right-hand-side term in (35) leads to

$$\left(\frac{dJ}{dy}\right)_{y=0} = \frac{J(0)}{\alpha+1}\left(\frac{d\lambda}{dy}\right)_{y=0} + \frac{\theta}{(\gamma_c-1)(\alpha+1)}. \tag{37}$$

Alternatively, this derivative may be found by differentiating (33), giving

$$\left(\frac{dJ}{dy}\right)_{y=0} = \xi_0 + Q(0)\left(\frac{d\lambda}{dy}\right)_{y=0}, \tag{38}$$

where

$$\xi_0 \equiv \left(\frac{dS}{dy}\right)_{y=0} + (\alpha+1)\left(\frac{dQ}{dy}\right)_{y=0}.$$

Hence, eliminating $(d\lambda/dy)_{y=0}$ between (37) and (38), and making use of (33), we have finally

$$\left(\frac{dJ}{dy}\right)_{y=0} = \xi_0 + \frac{(\alpha+1)Q(0)}{S(0)}\left[\xi_0 - \frac{\theta}{(\gamma_c-1)(\alpha+1)}\right]. \tag{39}$$

The slopes $(dS/dy)_{y=0}$ and $(dQ/dy)_{y=0}$ can be obtained numerically from the definitions of S and Q; $S(0)$ and $Q(0)$ can be computed directly.

4. Simplification for strong waves

A blast wave is said to be 'strong' when $M_s \to \infty$, $R \to 0$, strictly, so that $y = M_s^{-2} \to 0$. For many purposes it is satisfactory when dealing with gas-phase blast waves to extend the strong wave assumption to Mach numbers as low as five or six. In this regime it is not necessary to integrate (35). Rather, $J \doteq J(0)$, readily calculated from (33) with $\lambda \doteq \lambda(0) = \alpha + 1$, can be used. Thus, since $J(0)$ and θ are finite, (36) becomes

$$\frac{R}{R_0} = \left[\frac{y}{J(0)}\right]^{1/(\alpha+1)}$$

or

$$M_s = \left[\frac{E_\alpha}{J(0)\,P_1 R^{\alpha+1}}\right]^{\frac{1}{2}}. \tag{40}$$

This simple closed-form equation suggests a direct comparison of the relative decay rates of strong gas-phase ($\omega_s = 0$) and two-phase ($\omega_s > 0$) blast waves. If both waves occur with the same values of E_α and P_1, then, at equal wave radii, the ratio of their shock front strengths will be

$$\nu \equiv \frac{M_{s_T}}{M_{s_G}} = \left[\frac{J_G(0)}{J_T(0)}\right]^{\frac{1}{2}}, \tag{41}$$

where the subscripts T and G refer to values for the two-phase and gas-phase quantities, and ν is the 'attenuation ratio'.

5. Results and discussion

Although a full parametric study has not been carried out, calculations were executed for two representative groups of parameters. The first group is characteristic of water droplets suspended in nitrogen gas at one atmosphere initial pressure and an initial temperature of 25 °C. The values are $\bar{C}_p = 1{\cdot}79$, $\bar{\gamma} = 1{\cdot}05$, and $\bar{L} = 19{\cdot}5$. The second group is characteristic of any of several hydrocarbon fuels, such as iso-octane, kerosene, gasoline, *n*-decane, and diethylcyclohexane, the droplets again being suspended in nitrogen gas at one atmosphere and 25 °C. In this case the approximate values are $\bar{C}_p = 1{\cdot}6$, $\bar{\gamma} = 1{\cdot}35$, and $\bar{L} = 2{\cdot}5$.

The qualitative nature of the results support intuition. In a two-phase blast wave, some of the deposited energy must be expended in order to overcome the heat of vaporization of the liquid droplets. The remaining energy is shared within the wave by both species. These two effects result in accelerated wave attenuation rates. At the same time, the densities and pressures within the two-phase blast wave are increased by the liquid mass loading.

Figures 2–4 compare the decay rates of two-phase planar, cylindrical, and spherical blast waves for the fuels in nitrogen. The equivalent decay curves for a cylindrical blast wave in water/nitrogen are shown on figure 5.

The magnitude of the effect of the presence of droplets on the blast wave attenuation rate is significant. For example, the planar blast wave of figure 2 decays to $M_s = 4$ at a dimensionless radius of $3{\cdot}75 \times 10^{-2}$ when no droplets are present ($\omega_s = 0$). However, with a liquid loading factor of $\omega_s = 0{\cdot}4$, the wave decays to $M_s = 4$ at $R/R_0 = 1{\cdot}48 \times 10^{-2}$, which represents about 40 % of the distance traversed by the gas-phase wave.

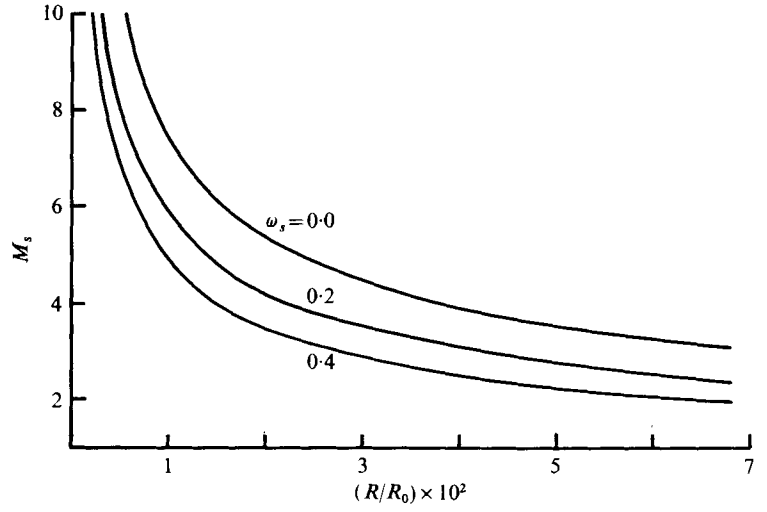

FIGURE 2. Decay curves, planar wave ($\alpha = 0$); $\overline{C}_p = 1{\cdot}6$, $\overline{\gamma} = 1{\cdot}35$, $\overline{L} = 2{\cdot}5$ (fuels), nitrogen carrier, $T_1 = 25\,^{\circ}\mathrm{C}$.

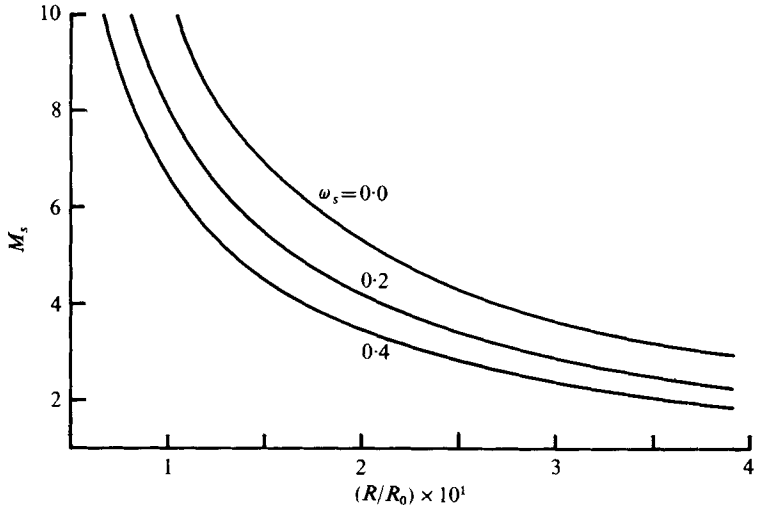

FIGURE 3. Decay curves, cylindrical wave ($\alpha = 1$); $\overline{C}_p = 1{\cdot}6$, $\overline{\gamma} = 1{\cdot}35$, $\overline{L} = 2{\cdot}5$ (fuels), nitrogen carrier, $T_1 = 25\,^{\circ}\mathrm{C}$.

Typical pressure, density, and absolute velocity profiles are shown on figure 6–8. The shapes of the two-phase profiles are similar to their gas-phase counterparts. However, owing to mass loading by the droplets, the pressures in two-phase blast waves are higher than in gas-phase waves. The difference is very significant for the case of $\omega_s = 0{\cdot}4$ illustrated in figure 6. For the same conditions, the density at the front of the two-phase blast wave shown on figure 7 is 2·3 times the gas-phase value, although it drops off more rapidly toward the centre of explosion. Absolute particle velocities are also higher in a two-phase wave, as can be seen on figure 8. It will be recalled that velocity profiles are linear by assumption.

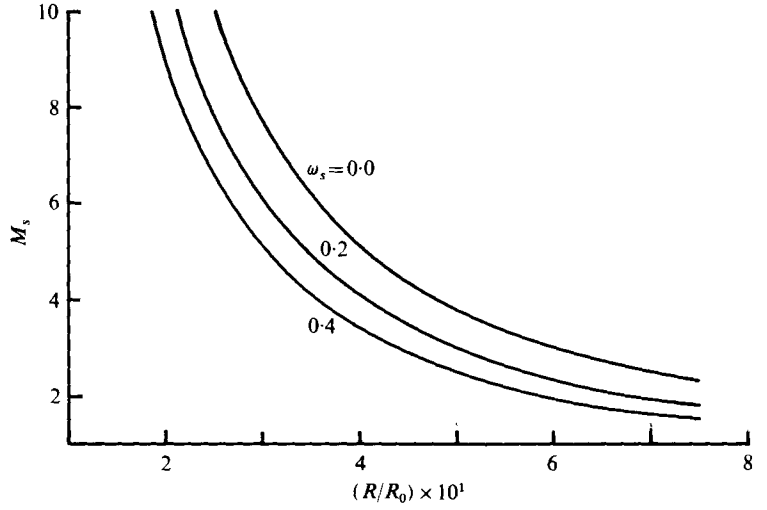

FIGURE 4. Decay curves, spherical wave ($\alpha = 2$); $\overline{C}_p = 1{\cdot}6$, $\overline{\gamma} = 1{\cdot}35$, $\overline{L} = 2{\cdot}5$ (fuels), nitrogen carrier, $T_1 = 25$ °C.

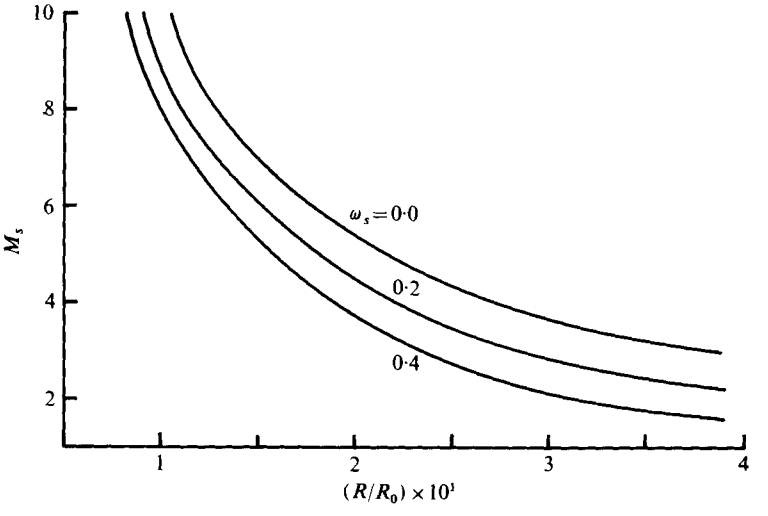

FIGURE 5. Decay curves, cylindrical wave ($\alpha = 1$); $\overline{C}_p = 1{\cdot}79$, $\overline{\gamma} = 1{\cdot}05$, $\overline{L} = 19{\cdot}5$, (water), nitrogen carrier, $T_1 = 25$ °C.

From these results it is not immediately clear whether the impulse imparted by the blast wave to the ground, or to a suspended body, will be larger or smaller when droplets are present initially. Although the wave attenuates more rapidly than it would without droplets present, it occurs with what can be substantially higher static and dynamic pressures throughout the shortened decay period.

Attentuation ratios for strong waves have been calculated and are presented as functions of loading factor on figure 9. For a given set of parameters the values were found to be very nearly equal in all geometries; only single average curves have therefore been given. Attenuation ratios should prove useful as a first-order means to

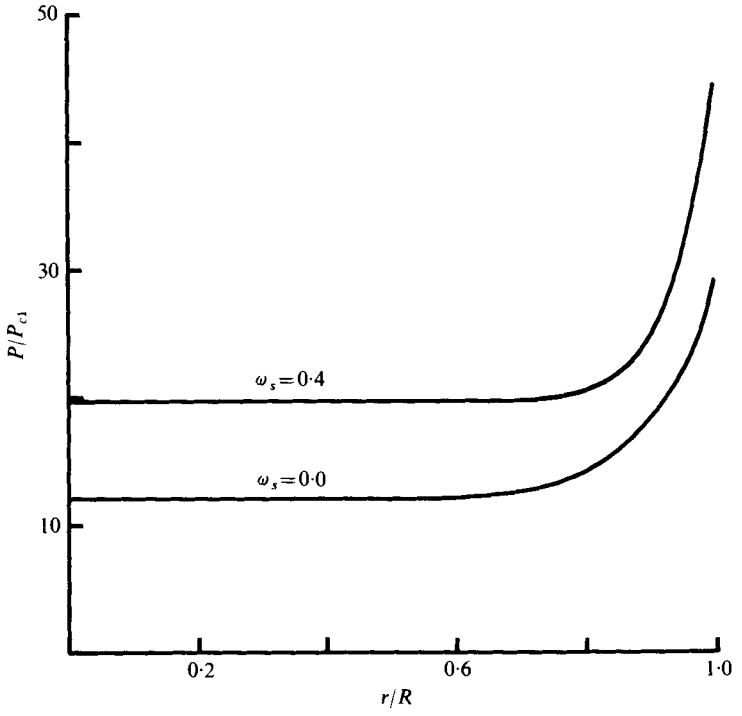

FIGURE 6. Pressure profiles at $M_s = 5$; $\alpha = 1$, $\bar{C}_p = 1{\cdot}6$, $\bar{\gamma} = 1{\cdot}35$, $\bar{L} = 2{\cdot}5$ (fuels), nitrogen carrier, $T_1 = 25\,^{\circ}\mathrm{C}$.

assess the effects of a spray on blast-wave decay rates, since these ratios can be quickly calculated.

The analysis of two-phase blast waves as presented in this paper was developed on the fundamental assumption that at any instant, the blast-wave radius is much larger than the distance behind the shock that is required for the complete change of phase of the liquid droplets. For this reason the shock and phase-change region have together been treated as a single discontinuity.

The interaction of a shock wave with a single non-reactive liquid droplet suspended in a gas has been described in some detail by a number of authors. After a shock wave has passed over the initially stationary droplet, finite droplet acceleration gives rise to a period during which a relative velocity exists between it and the shocked gas. Even for shocks of moderate strength, this relative velocity enormously increases the droplet disintegration rate.

Using results given by Ranger & Nicholls (1972), the approximate distance traversed by the shock during the disintegration period is

$$x_s \doteq 5D\left(\frac{u_1}{u_2}\right)\left(\frac{\rho_l}{\rho_{c2}}\right)^{\frac{1}{2}}, \tag{42}$$

whereas the distance that the droplet itself is displaced in the same time interval is

$$x_D \doteq 25D, \tag{43}$$

where D is the initial droplet diameter, ρ_l is the condensed-phase liquid density, and

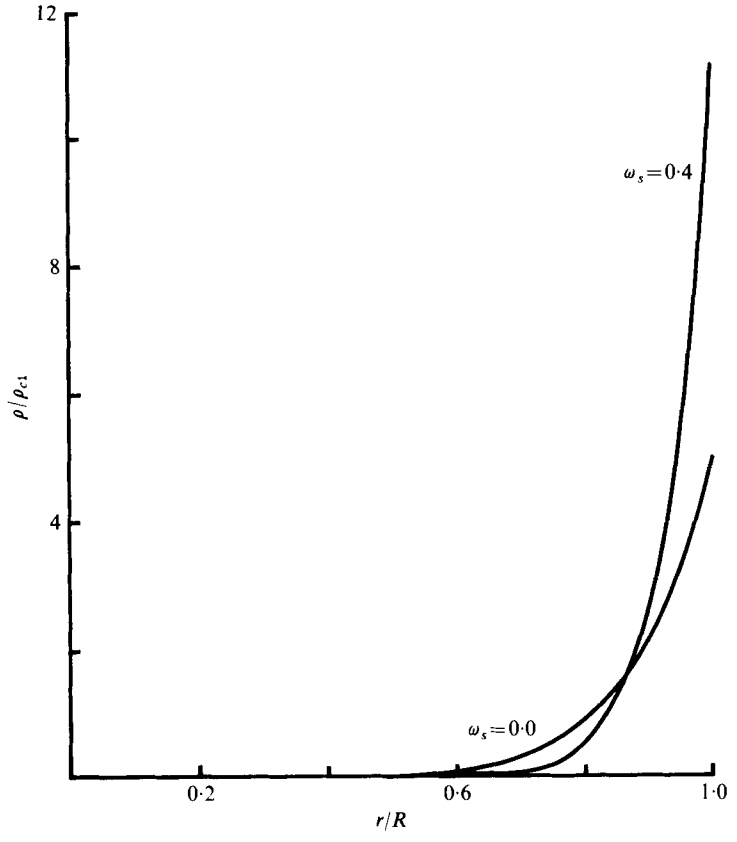

FIGURE 7. Density profiles at $M_s = 5$; $\alpha = 1$, $\bar{C}_p = 1{\cdot}6$, $\bar{\gamma} = 1{\cdot}35$, $\bar{L} = 2{\cdot}5$ (fuels), nitrogen carrier, $T_1 = 25\,^{\circ}\mathrm{C}$.

point 2 is located just behind the shock itself, as shown on figure 1. The length of the phase-change region, x_B, is then approximately

$$x_B = x_S - x_D. \tag{44}$$

Now, it is required by the present analysis that $x_B/R < \delta$, where $\delta \to 0$. Using (42)–(44) and simplifying, this condition can be written as

$$\left(\frac{D}{R_0\delta}\right)_{\max} = \bar{R}\,5^{-1}\left[\frac{(\rho_l\rho_{c2})^{\frac{1}{2}}}{\rho_{c2}-\rho_{c1}} - 5\right]^{-1}, \tag{45}$$

where $\bar{R} = R/R_0$ is the dimensionless wave radius. Since the rise in density is finite across a simple shock and since $\bar{R} \to 0$ as $M_s \to \infty$, it is clear that the maximum allowable drop size is always zero at $R = 0$. The maximum allowable drop size is also zero as $M_s \to 1$ since in that limit no change of phase occurs at all.

Thus the primary assumption for the simplified structure of a two-phase blast wave fails, except for infinitesimal drop sizes, at both the very strong and very weak limits. However, for intermediate-strength waves, realistic droplet sizes can be accommodated. For example, in spherical geometry ($\alpha = 2$), with $P_1 = 1$ atm, $T_1 = 25\,^{\circ}\mathrm{C}$, and $E_\alpha = 10^6$J (the equivalent of 200 g of TNT), the maximum drop size for one of the fuels

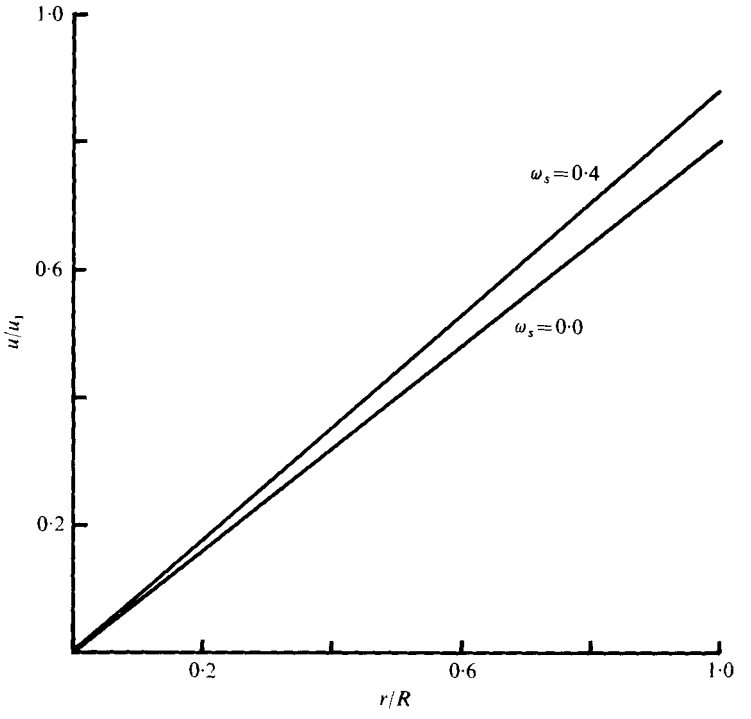

FIGURE 8. Particle velocity profiles at $M_s = 5$; $\alpha = 1$, $\overline{C}_p = 1{\cdot}6$, $\overline{\gamma} = 1{\cdot}35$, $\overline{L} = 2{\cdot}5$ (fuels), nitrogen carrier, $T_1 = 25\,°\mathrm{C}$.

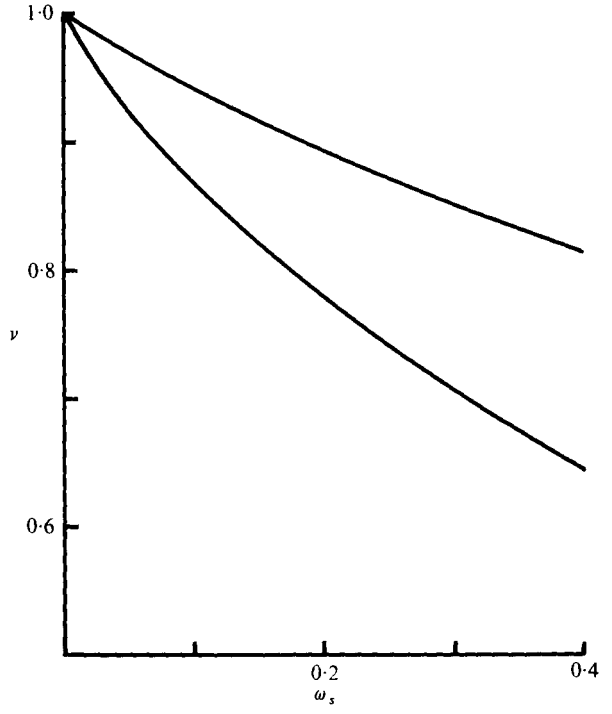

FIGURE 9. Attenuation ratio *vs.* loading factor. Upper curve, $\overline{C}_p = 1{\cdot}79$, $\overline{\gamma} = 1{\cdot}05$, $\overline{L} = 19{\cdot}5$ (water); lower curve, $\overline{C}_p = 1{\cdot}6$, $\overline{\gamma} = 1{\cdot}35$, $\overline{L} = 2{\cdot}5$ (fuels); both curves, nitrogen carrier, $T_1 = 25\,°\mathrm{C}$.

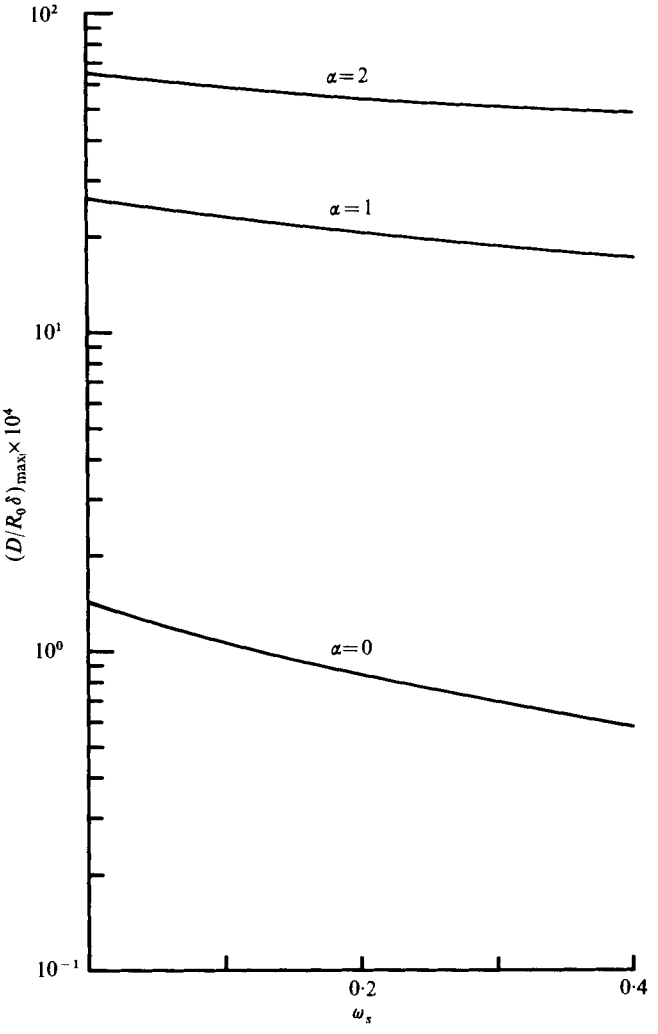

FIGURE 10. Maximum dimensionless drop size *vs.* loading factor at $M_s = 10$; $\overline{C}_v = 1{\cdot}6$, $\overline{\gamma} = 1{\cdot}35$, $\overline{L} = 2{\cdot}5$ (fuels), nitrogen carrier, $T_1 = 25\,^{\circ}\mathrm{C}$.

in nitrogen at $M_s = 10$ is about $520\,\mu$m, using $\delta = 0{\cdot}05$. This maximum drop *diameter* increases with decreasing Mach number until $M_s \sim 2$, then again decreases to zero as $M_s \to 1$. Its largest value is about one order of magnitude greater than that at $M_s = 10$. The maximum allowable drop size also increases with increasing deposited energy. Values of $(D/R_0\delta)_{max}$, calculated from (45), are plotted on figure 10.

A second important assumption in this analysis is that the 'approximate' shock relations, (10)–(12), can be used in place of the 'exact' relations, (7)–(9). The largest error between these two sets of equations occurs in the shock-relative velocity ratio, $\hat{u}_3/u_1$. This error is plotted on figure 11 for $\omega_s = 0{\cdot}4$. As can be observed, the error is reasonably small for the fuels group to Mach numbers as low as $M_s = 2$. The error with water droplets is however considerably higher and is probably excessive for Mach numbers less than four for the case shown. Since these errors decrease to zero at all

Mach numbers as $\omega_s \to 0$, the maximum tolerable error in a particular application will dictate either the minimum wave strength or the maximum loading factor for which this assumption can be retained.

The first of the two Sakurai assumptions that have been adopted in this paper is $f \propto x$. Particle velocity profiles in gas-phase blast waves are in fact reasonably linear at high Mach numbers and this generally remains an acceptable approximation for Mach numbers as low as about three. However, this assumption clearly excludes any realistic description of the final stages of wave decay where the significant feature is a backflow of gas towards the explosion centre. The 'linear particle velocity' assumption is extended to two-phase blast waves without further justification.

The second Sakurai assumption, that $\lambda y\, \partial h/\partial y \ll (f-x)\, \partial h/\partial x$, is somewhat more tenuous. That assumption is needed in order to obtain a simple form for $h(x, y) \equiv P/P_{c1}$ through an integration of (15). When this is done (22) results,

$$h = h_0(y)\, x^m.$$

If $\lambda y\, \partial h/\partial y$ is retained in (15), rearrangement of that equation gives

$$\frac{1}{h}\frac{\partial h}{\partial x} + \frac{\lambda y}{x(f_0-1)\,h}\frac{\partial h}{\partial y} = \frac{f_0(\alpha+1)}{x(1-f_0)},$$

where $f = f_0 x$ has been used. Multiplying by dx and integrating leads to

$$\frac{h}{h_0 x^m} = \Gamma(x, y),$$

where

$$\Gamma \equiv \exp\left[-\int \frac{\lambda y}{x(f_0-1)\,h}\left(\frac{\partial h}{\partial y}\right) dx\right].$$

The form $h = h_0 x^m$ will thus be a satisfactory representation of the density distribution within the blast wave if $\Gamma \doteq 1$.

Approximate values of Γ were calculated using $h = h_0 x^m$ and performing the indicated integration. This results in

$$\Gamma = x^{\beta},$$

where

$$\beta \equiv \frac{\lambda y C}{f_0-1}\left[\frac{\alpha+1}{2(1-f_0)^2}\ln x + \frac{\phi}{(Cy+\alpha_2)^2 h_0}\right],$$

and

$$C \equiv \alpha_2 \mu/\alpha_1 \phi.$$

The values of Γ calculated in this way are in fact unity at $x = 1$ and at $y = 0$. At other (x, y) the departure from unity is typically significant. The greatest errors occur for $x < 0{\cdot}7$, a regime in which (except for low Mach numbers not presently treated) the values of h are very small. Most of the important variation in density occurs for $x > 0{\cdot}7$ as can be seen on figure 7. It is not likely that imprecision in density values for $x < 0{\cdot}7$ would seriously compromise the remainder of the solution.

Unfortunately, even for $0{\cdot}7 < x < 1$, values of Γ characteristically vary between 0·85 and 1·15. Hence, except for strong waves, it appears that neglecting $\lambda y\, \partial h/\partial y$ in (15) can introduce non-trivial error, particularly in the density and temperature profiles at lower Mach numbers. While this problem is certainly of some concern, it is encouraging to note that for the gas-phase blast waves analysed with this approximation by Sakurai (1965), the predicted wave decay rates agree quite favourably with more accurate solutions.

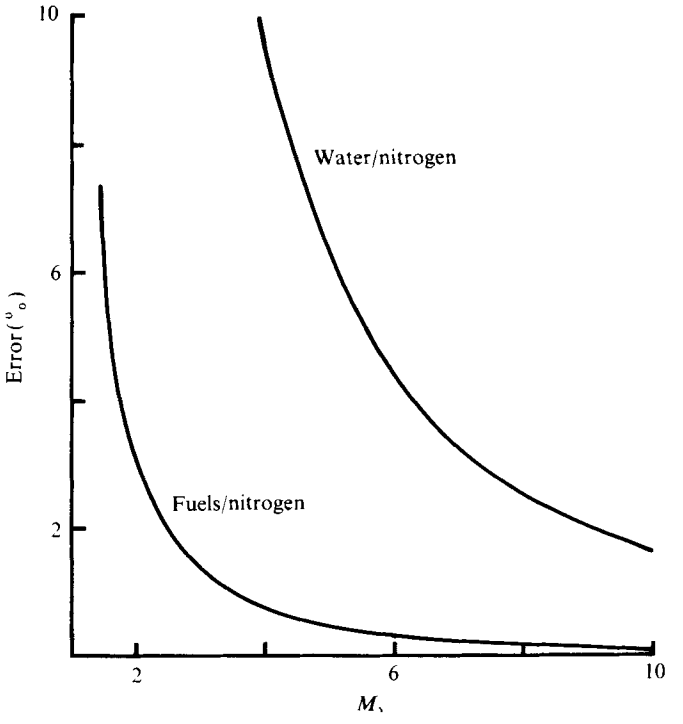

FIGURE 11. Error in $\hat{u}_3/u_1$ between 'exact' and 'approximate' shock discontinuity solutions, $\omega_s = 0{\cdot}4$.

6. Conclusions

An objective in this study has been to provide a physically reasonable description of a two-phase blast wave cast in an accessible analytic format. Use of the results requires the integration of a single ordinary differential equation, (35). If the strong-wave approximation is used, no integration at all is required.

However, this simplified formulation cannot acceptably describe the blast-wave characteristics either at very high Mach numbers ($R \to 0$) or at very low Mach numbers ($R \to \infty$). In the earliest stages of decay, the droplet breakup and evaporation zone width is large compared with the wave radius. It is likely that during this period the drops have little effect on the wave which therefore exhibits gas-phase blast-wave behaviour. As the wave expands further, the breakup width first becomes comparable to, and then much smaller than the wave radius (for sufficiently large energy deposition or sufficiently small droplets). Since the integration of (35) begins at $y = 0$, errors in that vicinity will persist throughout the remaining solution. Further study will be required to reveal the extent of this effect.

When the wave has decayed to low Mach numbers the droplet breakup distance again becomes comparable to the wave radius. At the same time the approximate shock solutions, (10)–(12), and the Sakurai assumptions, $f \propto x$ and $\partial y\, \partial h/\partial y \ll (f-x)\, \partial h/\partial x$, all become unacceptably inaccurate. The approximate shock solutions also become progressively less accurate with increasing loading factor.

In view of all these observations it would appear that the present analytical treatment can be implemented with reasonable accuracy for wave strengths falling typically in the range $4 < M_s < 15$, loading factors less than $\omega_s \doteq 0{\cdot}4$, and values of $D/R_0\delta$ less than those given on figure 10. This recommendation should be regarded as applicable only to spray/carrier combinations with values of γ_c, $\bar{C}_p$, $\bar{\gamma}$, and $\bar{L}$ near those of the representative calculations. Above $M_s \doteq 15$ it is likely that the conventional, strong gas-phase blast-wave solution will yield the better approximation. The upper limit on M_s depends on drop size and can be increased with reduced values of $D/R_0\delta$.

This work was supported in part by U.S. Army Explosives Laboratory, Picatinny Arsenal, Contract No. DAAA 21-73-C-0571 under the direction of N. Slagg, and in part by a grant from E. I. DuPont De Nemours and Company, Inc. Early work was conducted at the University of Michigan Gas Dynamics Laboratories, Ann Arbor, in collaboration with J. A. Nicholls.

REFERENCES

Bach, G. G., Knystautas, R. & Lee, J. H. 1971 Initiation criteria for diverging gaseous detonations. *13th Symp. (Int.) on Combustion, Combustion Inst., Pittsburgh*, p. 1097.

Dabora, E. K. 1972 Variable energy blast waves. *A.I.A.A. J.* **10**, 1384.

Korobeinikov, V. P. 1971 Gas dynamics of explosions. *Ann. Rev. Fluid Mech.* **3**, 317.

Ranger, A. A. & Nicholls, J. A. 1972 Atomization of liquid droplets in a convective stream. *Int. J. Heat Mass Transfer* **15**, 1203.

Sakurai, A. 1965 Blast wave theory. In *Basic Developments in Fluid Dynamics*, vol. I (ed. M. Holt), p. 309. Academic Press.

Sedov, L. I. 1959 *Similarity and Dimensional Methods in Mechanics*. Academic Press.

Treve, Y. M. & Manley, P. P. 1972 A point explosion in an arbitrary atmosphere. *J. Fluid Mech.* **55**, 737.

Woolfolk, R. W. & Ablow, C. M. 1974 Dependence of the blast wave from an explosion on the energy release rate. *15th Symp. (Int.) on Combustion, Combustion Inst., Pittsburgh*, unpublished preprint.